

TABLE I. Experimentally determined parameters for the neutron photoproduction cross sections σ_m , maximum value of cross sections; E_m , energy at which maximum occurs; DSR, classical dipole-sum rule limit; Γ_0 twice the energy from half-maximum on low-energy side of curve to E_m , Γ_{Lor} width used to fit the Lorentz curve

| | σ_m mb | E_m MeV | $\int_{Thr}^{80} \sigma dE$ MeV-b | DSR MeV-b | Γ_0 MeV | Γ_{Lor} MeV |
|------------------------------|------------------|--------------|--------------------------------------|--------------|-------------------|-----------------------|
| Uncorrected for multiplicity | | | | | | |
| La | 315±15 | 14.8±0.4 | 1.76 | 2.02 | | |
| Pr | 305±10 | 14.8±0.4 | 1.74 | 2.06 | | |
| Corrected for $(\gamma, 2n)$ | | | | | | |
| La | 304 | 14.5 | 1.36 | 2.02 | 3.2±0.2 | 3.3 |
| Pr | 305 | 14.8 | 1.47 | 2.06 | 4.0±0.2 | 3.3 |

line in each figure is a result of a Lorentz curve fitting to the low-lying points on the low-energy side of the peak.

Table I gives the results of the maximum cross section, the energy at which the peak occurs, and the integrated cross section to 30 MeV for both the raw and corrected data as well as the results of the classical dipole-sum rule calculation for these elements. Also included are the measured half-widths of the curves: Γ_0 gives the value of twice the energy from one half-maximum on the low-energy side to the peak found from the corrected data; Γ_{Lor} is the width of the Lorentz curve used to fit each set of corrected data.

The integrated cross sections to 30 MeV are lower than those obtained from the classical Levinger and Bethe sum rule, but the cross section curves indicate that some dipole strength exists above 30 MeV. Each cross section displays a similar narrow resonance region in agreement with the prediction of hydrodynamic model for closed shell nuclei, but there is evidence for more complicated resonance phenomena, especially in praseodymium, and both cross sections deviate from the shape of a single Lorentz curve fitting.

Cross Sections and Isomer Ratios for the Isomeric Pair Y^{90g} and Y^{90m} in the $Rb^{87}(\alpha, n)$ and $Y^{89}(d, p)$ Reactions*

CLYDE RILEY AND BRUNO LINDER

Department of Chemistry, Florida State University, Tallahassee, Florida

(Received 22 August 1963, revised manuscript received 10 January 1964)

Excitation functions and cross section ratios for the isomeric pair Y^{90g} and Y^{90m} produced from Rb^{87} by (α, n) reaction and from Y^{89} by (d, p) reaction were measured from 11–18 and 5–12 MeV, respectively. The isomer ratios produced in (d, p) reaction are approximately an order of magnitude smaller than those obtained by (α, n) reaction; the total cross sections for both reactions are comparable. The differences in the isomer ratio curves are accounted for by differences in mechanism. The experimental isomer ratios obtained in the (α, n) reaction are compared with the predicted values calculated in the manner of Huizenga and Vandenbosch. The results are discussed.

I. INTRODUCTION

IN recent years, a great deal of attention has been focused on the experimental and theoretical aspects of nuclear reactions in which isomers are produced.^{1–6} An exact prediction of a nuclear reaction can, in general, not be attempted without having detailed knowledge of the structure of the nucleus. However, when a process is known to proceed via the formation of a compound nucleus and the energy of the impinging particle is

sufficiently great, it is possible to make certain predictions regarding the cross section which will depend only upon the charge and mass of the target nucleus and the charge and energy of the incident particle. Isomer ratios, however, require a somewhat more detailed knowledge of the decay process in which angular momentum is now a more important entity. Several explanations have been offered to account for the observed isomer ratios, all of which invoke the law of conservation of angular momentum and make explicit use of the spin dependence of energy states. The most quantitative calculations were carried out by Huizenga and Vandenbosch³ and by Need.⁶

In this work we have determined the cross sections and isomer ratios for the reactions $Rb^{87}(\alpha, n)$, $Y^{90g, 90m}$, and $Y^{89}(d, p)Y^{90g, 90m}$. These reactions are of particular interest because the same final states are obtained by

* Supported by the U. S. Atomic Energy Commission.

¹ J. W. Meadows, R. M. Diamond, and R. A. Sharp, Phys. Rev. **102**, 190 (1956).

² B. Linder and R. A. James, Phys. Rev. **114**, 322 (1959).

³ J. R. Huizenga and R. Vandenbosch, Phys. Rev. **120**, 1305, 1313 (1960).

⁴ G. R. Choppin and T. Sikkland, J. Inorg. Nucl. Chem. **21**, 201 (1961).

⁵ J. L. Need and B. Linder, Phys. Rev. **129**, 1298 (1963).

⁶ J. L. Need, Phys. Rev. **129**, 1302 (1963).

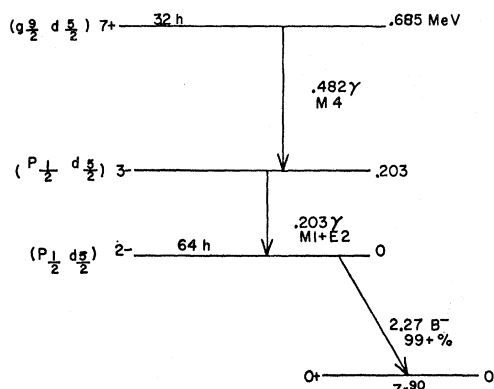


FIG. 1. Level scheme for Y^{90g} and Y^{90m} . Taken from R. L. Heath, J. E. Cline, C. W. Reich, E. C. Yates, and E. H. Turk, Phys. Rev. **123**, 908 (1961).

two different mechanisms, the former representing a reaction which proceeds predominantly via compound nucleus formation, the latter a stripping reaction. Widely different isomer ratios are expected for these two mechanisms. Few isomer ratios for reactions of these types have been studied. Isomer ratios of (d,p) reactions were measured by Huizenga and Vandenbosch³ for $Hg^{197g,197m}$ at 11 MeV and by Zherebtsova *et al.*⁷ for $Zn^{69g,69m}$ between 2 and 10 MeV. Also, isomer ratios have been reported between 6 and 40 MeV for the $K^{41}(\alpha,n)Sc^{44m,g}$ reaction.⁸ In the present work, the cross sections for the (α,n) reaction were measured from 11–18 MeV and the cross sections for the (d,p) reaction from 5–12 MeV. The experimental isomer ratios for the (α,n) reaction were compared with the theoretical predictions, calculated in the manner of Huizenga and Vandenbosch.

II. EXPERIMENTAL METHOD

A. Chemical Procedure

1. $Rb^{87}(\alpha,n)Y^{90g,90m}$

The rubidium targets were prepared by evaporating high-purity RbCl upon aluminum backings with a thickness of 1 mg/cm² or less. The targets were then individually bombarded with 11–18-MeV alpha particles from the Florida State University Tandem Van de Graaff accelerator.

After irradiation, the targets were dissolved in HCl; yttrium, strontium, and barium carriers were added and the solution was made strongly basic with NaOH to remove aluminum. After washing, the precipitate was dissolved in a small amount of concentrated HNO₃, strontium and barium carriers were again added and then precipitated as nitrates with fuming nitric acid. The cleaning of barium and strontium was repeated

⁷ K. I. Zherebtsova, T. P. Makasova, A. Nemilov, and B. L. Funshtein, Zh. Eksperim. i Teor. Fiz. **35**, 1355 (1958) [English transl.: Soviet Phys.—JETP **8**, 947 (1959)].

⁸ T. Matsuo and T. T. Sugihara, Can. J. Chem. **39**, 697 (1961).

and the remaining solution was evaporated to dryness. The residue of yttrium salts was dissolved in a H₂SO₄, (NH₄)₂SO₄, H₂O₂ and oxalic acid mixture, precipitated as the oxalate, filtered, and prepared for counting. The chemical yield was determined after counting by ignition of the oxalate to yttrium oxide.

2. $Y^{89}(d,p)Y^{90g,90m}$

The yttrium targets were prepared by evaporating high-purity yttrium metal upon aluminum backings with a thickness of 0.2 mg/cm² or less. The targets were then individually bombarded with 5–12-MeV deuterons from the Florida State University Tandem Van de Graaff accelerator.

Following irradiation, the targets were dissolved in HCl, standard yttrium carrier was added and the solution was made strongly basic to remove aluminum. After washing with NH₄OH, the precipitate was dissolved in HCl and zirconium carrier was added and then removed by precipitating the yttrium as YF₃ with HF. The precipitate was washed and dissolved in a small amount of a mixture of saturated boric acid and concentrated nitric acid. The solution was then diluted with H₂O, the yttrium precipitated as an oxalate, filtered, dried, and mounted in the standard way.

B. Counting

The prepared samples were gamma counted as soon as possible flat against the aluminum shield of a 3- \times 3-in. NaI scintillation crystal. After a period of ten half-lives (\sim 32 h), the samples were beta counted with a lead shielded calibrated Geiger-Müller counter.

Displayed in Fig. 1 is the level scheme for Y^{90g} and Y^{90m} . Crossover to Zr^{90} from the 685-keV level is very small, and decay of the ground state via the 2.27-MeV β^- to the 0+ level of Zr^{90} is 99% or greater. Because of the simplicity of the level scheme, very little decay scheme error will be involved.

Since natural RbCl was used as the target material for the alpha bombardments, other isotopes of yttrium

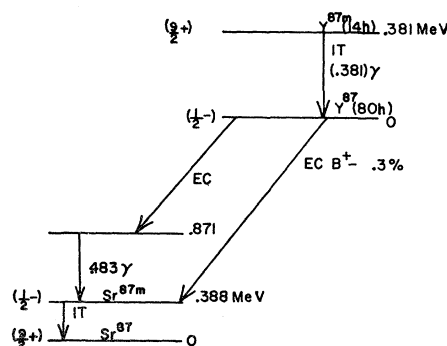


FIG. 2. Level scheme for Y^{87g} and Y^{87m} . Taken from D. Strominger, J. M. Hollander, and G. T. Seaborg, Rev. Mod. Phys. **30**, 661 (1958).

will be produced that cannot be radiochemically separated. The only interfering isotope was $Y^{87g,87m}$, which resulted from the reaction $Rb^{87}(\alpha,2n)Y^{87g,87m}$. Reference to the decay scheme in Fig. 2 shows interference from a 0.483-MeV gamma, and the conversion electrons from the 0.381- and 0.388-MeV gammas. However, these difficulties were overcome by a "sum peak" determination of the Y^{90m} activity and by using 140 mg/cm² of aluminum absorber to eliminate the conversion electrons from the ground-state beta count.

Corrections were made to the 482-keV peak and 685-keV "sum peak" for bremsstrahlung produced by conversion electrons and the 2.27-MeV beta. In most instances the corrections were found to be negligible at the count rates encountered.

III. DATA TREATMENT

In order to decrease the bombardment time, the gamma counting of the 0.685-MeV isomeric state was done with the best geometry possible. This resulted in the creation of a sizable sum peak which had good counting statistics making it possible to use the sum peak for determining the isomeric activity.

The probability of "summing" is proportional to the product of the efficiencies of the summing photons, corrected by angular correlation and coincidence factors. Referring to the decay scheme, Fig. 1, and using conversion coefficients of 0.11 and 0.03 for the 0.482-MeV photon (γ_1) and 0.203-MeV photon (γ_2), respectively,^{9,10} it is seen that the coincidence factor is 0.97. The angular correlation factor $\bar{\omega}(\theta)$ which can be evaluated by the methods of Rose¹¹ was determined experimentally.

Adopting the notation of Lazar and Klema,¹² for every γ_1 , which is detected with complete energy dissipation in the scintillator, the probability of γ_2 being detected with complete energy dissipation ρ_2 is

$$\rho_2 = \epsilon_2 R_2 \bar{\omega}(\theta) g_{2/1}, \quad (1)$$

where ϵ_2 is the total absolute efficiency of the crystal for detection of γ_2 , R_2 , the photopeak to total ratio, $g_{2/1}$ the number of γ_2 in coincidence with γ_1 , and $\bar{\omega}(\theta)$ the angular distribution function of the two photons integrated over the face of the crystal. The detection rate of γ_1 , N_{1f} is given by

$$N_{1f} = N_1^0 \epsilon_1 R_1 = \frac{N_1}{1 - \epsilon_2 \bar{\omega}(\theta) g_{2/1}}, \quad (2)$$

where N_1^0 is the emission rate of the source of γ_1 , ϵ_1 the total absolute efficiency of γ_1 , R_1 the peak to total ratio of γ_1 and N_1 the area under the photo peak of γ_1 when summing is present. Thus, the area under the coincident

sum peak $N_{c.s.}$ will be given by

$$N_{c.s.} = N_1^0 \epsilon_1 R_1 \epsilon_2 R_2 \bar{\omega}(\theta) g_{2/1} + N_J \quad (3a)$$

or

$$N_{c.s.} = \frac{N_1 \epsilon_2 R_2 \bar{\omega}(\theta) g_{2/1}}{1 - \epsilon_2 \bar{\omega}(\theta) g_{2/1}} + N_J, \quad (3b)$$

where N_J is a rate which represents the statistical probability of the two transitions occurring within resolving time. N_J was found to be negligible. From the measured value of the area of the sum peak, taken from the spectra where there was no interference from $Y^{87g,87m}$, the area of the corrected 0.482-MeV photopeak, the coincidence rate, and efficiencies,¹³ $\bar{\omega}(\theta)$ could be evaluated and was found to have a value of 0.93. This value of $\bar{\omega}(\theta)$ was checked by preparing a point source which was counted with summing flat against the crystal shield, and counted at 10 cm with negligible summing. Comparison of N_1^0 obtained by counting the sample against the crystal shield [as evaluated by (3a)] with N_1^0 evaluated from the usual spectral analysis for the 0.482-MeV photopeak counted at 10 cm gave agreement within 3%. Also when the sample is placed against the crystal shield it creates nearly π geometry; it is therefore reasonable to assume that $\bar{\omega}(\theta)$ should approach unity as it does.

After correcting for decay the cross section for the isomeric production can be calculated by the usual bombardment equation

$$A_m^0 = \eta \sigma_m f (1 - e^{-\lambda_m t}), \quad (4)$$

where A_m^0 is the disintegration rate at the end of the bombardment, η is the target thickness in atoms/cm², σ_m the isomeric cross section, f the intensity of the bombarding beam, λ_m the isomeric decay constant, and t the bombardment time.

For the ground state, it can be shown that the disintegration rate at the end of the bombardment A_g^0 is given by

$$A_g^0 = \frac{\lambda_g A_m^0}{\lambda_g - \lambda_m} (e^{-\lambda_m t} - e^{-\lambda_g t}) + A_g^0 e^{-\lambda_g t}, \quad (5)$$

where A_g is the disintegration rate of the ground state at the time of the beta count and λ_g is the decay constant for the ground state. From A_g^0 the cross section for the ground state σ_g can be calculated with

$$A_g^0 = \eta f \left[(\sigma_m + \sigma_g) (1 - e^{-\lambda_g t}) + \frac{\lambda_g \sigma_m}{\lambda_g - \lambda_m} (e^{-\lambda_g t} - e^{-\lambda_m t}) \right], \quad (6)$$

which can be derived from the standard decay and rate production expressions.

⁹ R. L. Heath, J. E. Cline, C. W. Reich, E. C. Yates, and E. H. Turk, Phys. Rev. **123**, 908 (1961).

¹⁰ L. Haskin and R. Vandenbosch, Phys. Rev. **123**, 184 (1961).

¹¹ M. E. Rose, Phys. Rev. **91**, 610 (1953).

¹² N. H. Lazar and E. D. Klema, Phys. Rev. **98**, 710 (1955).

¹³ R. L. Heath, Atomic Energy Commission Report No. I DO-16408, 1957 (unpublished).

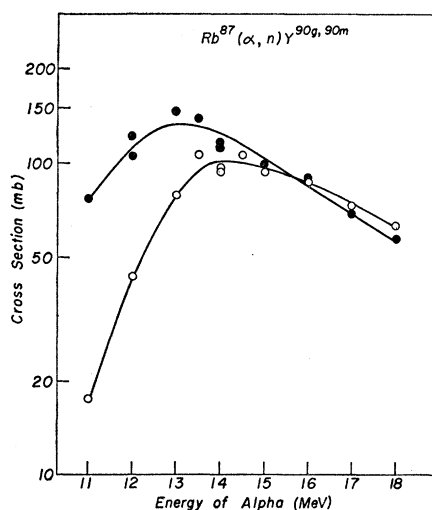


FIG. 3. Excitation function for $\text{Rb}^{87}(\alpha, n)\text{Y}^{90g, 90m}$ represented as solid dots, and excitation function for $\text{Rb}^{87}(\alpha, n)\text{Y}^{90m}$ shown as open circles.

IV. EXPERIMENTAL RESULTS

A. $\text{Rb}^{87}(\alpha, n)\text{Y}^{90g, 90m}$

The excitation function for formation of the ground (2^-) state and isomeric (7^+) state are displayed in Fig. 3. The error in the cross sections is estimated to be $\pm 15\%$ for the metastable state and $\pm 25\%$ for the ground state. Variations of energy from the plotted values can only take place toward lower energies, since the energy of the alpha particles striking the target surface is known very accurately.

Table I lists the cross sections for the two states from 11 to 18 MeV. The maximum deviation of the tabulated energies was calculated to be approximately 25 keV toward lower energy. Also tabulated are the isomer ratios for the reaction and their estimated errors.

In the determination of the isomer ratios, errors in beam intensity, target thickness, target uniformity, and chemical yield cancel. The only errors detrimental to the ratios are counting errors. Since the 685-keV state was gamma counted by a scintillation counter, and the ground-state beta counted with a Geiger-Müller counter, the errors involved in the determination of counter efficiencies will not cancel, but compound. The calculated errors in the isomer ratios are based on an estimated error of $\pm 10\%$ for the activity (not cross section) of the isomeric state and $\pm 20\%$ for the activity of the ground state.

Figure 4 displays the isomer ratios as a function of energy. Also shown in Fig. 4 are the calculated isomer ratios for which comment is reserved until the discussion.

B. $\text{Y}^{89}(d, p)\text{Y}^{90g, 90m}$

Displayed in Fig. 5 are the excitation functions for the ground and isomeric states, respectively. Since

TABLE I. Cross sections and isomer ratios for $\text{Rb}^{87}(\alpha, n)\text{Y}^{90g, 90m}$.

| MeV energy | σ_m (mb) | σ_g (mb) | $\frac{\sigma_m}{\sigma_g}$ | $\frac{\sigma_m}{\sigma_m + \sigma_g}$ |
|------------|-----------------|-----------------|-----------------------------|--|
| 11 | 17.5 | 77.4 | 0.23 ± 0.05 | 0.18 ± 0.03 |
| 12 | 39.8 | 105.5 | 0.38 ± 0.08 | 0.27 ± 0.05 |
| 12 | 43.4 | 121.0 | 0.36 ± 0.08 | 0.26 ± 0.05 |
| 13 | 79.0 | 145.5 | 0.54 ± 0.12 | 0.35 ± 0.06 |
| 13 | | | 0.60 | 0.38 |
| 13.5 | 107.5 | 138.2 | 0.78 ± 0.17 | 0.44 ± 0.07 |
| 14 | 94.0 | 112.4 | 0.84 ± 0.19 | 0.46 ± 0.08 |
| 14 | 96.1 | 116.4 | 0.82 ± 0.18 | 0.45 ± 0.07 |
| 14.5 | 106.1 | | | |
| 15 | 93.6 | 99.8 | 0.94 ± 0.21 | 0.48 ± 0.07 |
| 16 | 86.2 | 88.3 | 0.98 ± 0.22 | 0.49 ± 0.07 |
| 17 | 73.3 | 69.5 | 1.05 ± 0.24 | 0.51 ± 0.08 |
| 18 | 63.9 | 57.8 | 1.10 ± 0.25 | 0.52 ± 0.08 |

essentially the same techniques were applied in the determination of the cross sections, errors are again estimated at $\pm 15\%$ and $\pm 25\%$ for the excited and ground states, respectively. (Degradation of the deuteron energy from the indicated values was negligibly small.)

Table II lists the cross sections for the excited and ground states from 5 to 12 MeV. Also listed for this reaction are the isomer ratios. The estimated errors for the ratios were obtained in a similar fashion as for the $\text{Rb}^{87}(\alpha, n)\text{Y}^{90g, 90m}$ reaction. A plot of the isomer ratio cross sections versus energy is shown in Fig. 6 for the reaction $\text{Y}^{89}(d, p)\text{Y}^{90g, 90m}$.

V. DISCUSSION

The experimental isomer ratio function for the $\text{Rb}^{87}(\alpha, n)\text{Y}^{90g, 90m}$ reaction is displayed in Fig. 4. At low energies the ground state, which has a spin of 2, is favored; as the energy increases the metastable state ($I=7$) becomes more populated. Consideration of angular momentum conservation requires that at low

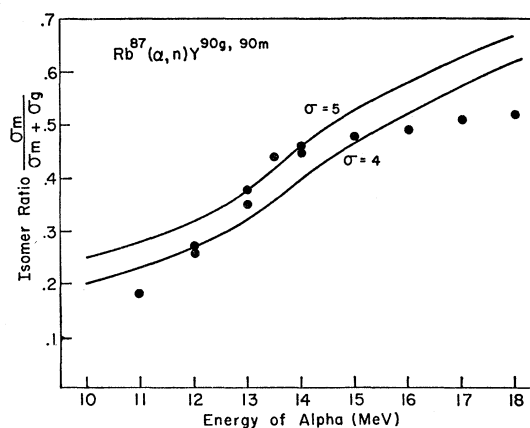


FIG. 4. Isomer ratios for $\text{Y}^{90g, 90m}$ pair produced by $\text{Rb}^{87}(\alpha, n)\text{Y}^{90g, 90m}$. Experimental values are represented by dots and calculated values as solid lines.

TABLE II. Cross sections and isomer ratios for $Y^{89}(d,p)Y^{90g,90m}$.

| Energy of deuteron MeV | σ_m (mb) | σ_g (mb) | $\frac{\sigma_m}{\sigma_g}$ | $\frac{\sigma_m}{\sigma_m + \sigma_g}$ |
|------------------------|-----------------|-----------------|-----------------------------|--|
| 5 | 1.6 | 63.1 | 0.025±0.006 | 0.025±0.005 |
| 6 | 4.4 | 127.0 | 0.035±0.008 | 0.033±0.007 |
| 7 | 8.8 | 173.3 | 0.051±0.011 | 0.048±0.010 |
| 8 | 10.3 | 156.1 | 0.066±0.015 | 0.062±0.013 |
| 8 | 12.5 | 194.4 | 0.064±0.015 | 0.060±0.013 |
| 9 | 16.2 | 191.1 | 0.085±0.019 | 0.078±0.016 |
| 9 | 16.3 | 209.3 | 0.078±0.017 | 0.072±0.015 |
| 10 | 16.9 | 177.7 | 0.095±0.022 | 0.087±0.018 |
| 10 | 16.7 | 176.9 | 0.094±0.022 | 0.086±0.018 |
| 11 | 18.1 | 177.9 | 0.102±0.023 | 0.092±0.019 |
| 11 | 17.3 | 175.5 | 0.098±0.022 | 0.090±0.019 |
| 12 | 16.3 | 150.2 | 0.108±0.024 | 0.098±0.020 |

energies (except in the vicinity of the threshold) the state having a spin closest to the target nucleus be populated; as the energy is increased the distribution of spins of the compound nucleus shifts to higher values thus increasing the previously unfavored state.

The results are compared with the theoretical predictions which were calculated in the manner of Huizenga and Vandenbosch. The solid lines shown in the figure represent the isomer ratio cross sections calculated for different values of the cutoff parameter σ , which appears in the formula for the spin distribution¹⁴

$$\rho(j) = \rho(0)(2j+1) \exp[-(j+\frac{1}{2})^2/2\sigma^2], \quad (7)$$

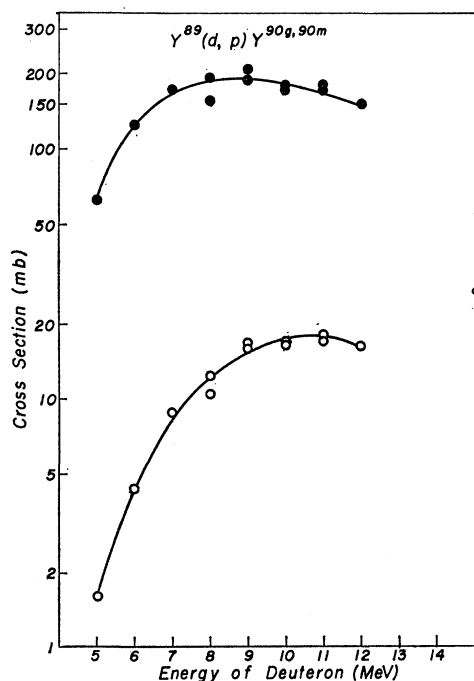


FIG. 5. Excitation function for $Y^{89}(d,p)Y^{90g}$ represented as solid dots, and excitation function for $Y^{89}(d,p)Y^{90m}$ shown as open circles.

¹⁴ See, for example, T. Ericson, Suppl. Phil. Mag. 9, 425 (1960).

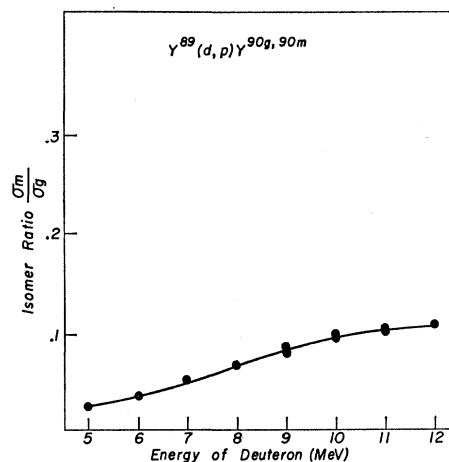


FIG. 6. Isomer ratios for $Y^{90g,90m}$ pair produced by $Y^{89}(d,p)Y^{90g,90m}$.

with the number of photons emitted from the residual nucleus taken to be 4 [where $\rho(j)$ is density of levels with spin j and $\rho(0)$ is density of levels with spin zero]. These calculations were carried out using the Huizenga and Igo¹⁵ optical potential alpha-particle transmission coefficients for Rb^{85} . The average neutron evaporation energy was taken to be 2 MeV. Square-well neutron transmission coefficients were used which were taken from Feld *et al.*¹⁶

The foregoing calculations are strictly valid only for a model which assumes compound nucleus mechanism and a spin distribution which is not affected by secondary-particle emission. The threshold for the $(\alpha,2n)$ reaction on Rb^{87} is approximately 10.5 MeV, which makes this reaction the predominate one over most of the experimental energy range studied. It is thus important to give consideration to the effect of two neutron emission upon the calculated (α,n) isomer ratios. The extent to which secondary neutron emission will have an effect upon the spin distribution which can deexcite by gamma emission can, in principle, be obtained by the method of the "average channel fraction" as developed by Grover.¹⁷ Unfortunately, Grover's average channel fraction can be calculated only from a knowledge of level spacings and radiation widths, information about which is almost totally lacking at the present time. Grover in a later paper proposed an approximation which entails preliminary averaging.¹⁸ When this approximation is applied to the case of isomers, the effect of spin fractionation on the ratio of their cross sections cancels.

It can be shown by physical arguments that spin

¹⁵ J. R. Huizenga and G. J. Igo, Atomic Energy Commission Report No. ANL-6373, 1961 (unpublished).

¹⁶ B. T. Feld, H. Feshbach, M. L. Goldberger, H. Goldstein, and V. F. Weisskopf, Atomic Energy Commission Report No. NYO-6363, 1951 (unpublished).

¹⁷ J. R. Grover, Phys. Rev. 123, 267 (1961).

¹⁸ J. R. Grover, Phys. Rev. 127, 2142 (1962).

fractionation will enhance the yield of the high spin state for the reaction under consideration.¹⁹ Opposed to this is the effect of direct interaction which would cause favoritism for the low-spin ground state. None of the calculated curves fit the experimental data well. Inclusion of spin fractionation would raise all the calculated curves with the $\sigma=4$ curve then describing the experimental isomer ratio function best. The flattening out of the experimental curve above 15 MeV is reminiscent of direct interaction behavior. Inclusion of direct interaction effects above 15 MeV would have the opposite effect, decreasing all calculated values, with $\sigma=5$ then giving the best description of the isomer ratio function. It is not possible from the present study alone to decide which of the two factors (if any or both) are responsible for the discrepancies between the experimental and calculated values. It would be necessary to study a reaction of this type below and above the $(\alpha,2n)$ threshold thoroughly before any definite conclusions can be drawn.

In sharp contrast to the (α,n) isomer ratio curve is the (d,p) curve²⁰ shown in Fig. 6. Here also, there is an initial increase in the isomer ratios up to about 9 MeV after which the curve appears to flatten out. However, it is to be noted that the initial increase in the (d,p) case is very small and as a result the isomer ratio changes little over the entire energy range as compared to the (α,n) ratios, regardless of the fact that the excitation energies are quite comparable. This is demonstrated even more clearly when σ_m/σ_g is compared for the two cases. This difference reflects a different mechanism, namely, one of stripping. In a stripping reaction, the proton is expected to carry off most of the energy and angular momentum, leaving the residual nucleus in a low state of angular momentum. This sharp contrast in behavior is characteristic only of the isomer ratio values and not of the over-all cross sections. Indeed, the total cross sections for the two reactions are comparable.

The low isomer ratio values obtained for the (d,p) reaction are in agreement with the low value obtained by Huizenga and Vandenbosch for the isomer pair

¹⁹ C. T. Bishop, Argonne National Laboratory Report No. ANL-6405, 121 ff, 1961 (unpublished).

²⁰ Although we are comparing σ_m/σ_g for the (d,p) reaction to $\sigma_m/(\sigma_m+\sigma_g)$ for the (α,n) reaction, reference to Table II will show the normalized values $\sigma_m/(\sigma_m+\sigma_g)$ for the (d,p) reaction to be even smaller and of very similar shape.

$\text{Hg}^{197g,197m}$ ($\sigma_m/\sigma_g=0.15$) at 11 MeV³; but are smaller than the results of Zherebtsova *et al.*⁷ for $\text{Zn}^{69g,69m}$. However, the shapes of the isomer ratio curves are very similar in the sense that the over-all change in σ_m/σ_g is very small over the comparable energy range. This difference in magnitude may be attributed to several differences in the reaction. Firstly, Zn^{69m} is a neutron level that can be populated directly while Y^{90m} is a proton level that can only be populated from higher energy states by cascading. Eby *et al.*²¹ have shown for the $\text{Zn}^{68}(d,p)\text{Zn}^{69g,69m}$ reaction, that the cross sections of the isomers obtained by *direct* production at 12 MeV are in the ratio of 0.4. They state further that this ratio is significantly greater than predicted by stripping theory. Secondly, if gamma cascading is considered, the amount of angular momentum required of the incoming neutron is much less for the Zn reaction than for the Y reaction. That is, for an equal number of emitted photons it would only be necessary to populate low J states of Zn^{69} which can decay to the isomeric state of spin $\frac{3}{2}$ whereas relatively higher J states would require population to produce the isomeric state of spin 7 in Y by decay.

Hence, neglecting magnitudes of (d,p) isomer ratios which will vary with the reaction, it would seem proper to conclude that the shape of the isomer plot of Fig. 6 is most important and is a general characteristic of stripping reactions. It would appear from the different shape of the (d,p) and (α,n) isomer ratio curves that isomer ratio studies could reveal details of a reaction process which could normally not be obtained from ordinary reaction studies. Experimental studies of isomer ratios could then hopefully be utilized to characterize reaction mechanisms where the latter are unknown.

ACKNOWLEDGMENTS

We are grateful to the U. S. Atomic Energy Commission for providing financial support for this research and to the U. S. Air Force for support of the FSU Tandem Van de Graaff accelerator. We also wish to thank Mrs. Carolyn Katz for help with chemical separation and Dr. John L. Need for helpful suggestions.

²¹ F. S. Eby, R. D. Hill, and W. K. Jenfschke, *Phys. Rev.* **93**, 925 (1954).